Journal of Biomedical Optics

SPIEDigitalLibrary.org/jbo

Terahertz sources

Pavel Shumyatsky
Robert R. Alfano

Terahertz sources

Pavel Shumyatsky and Robert R. Alfano
City College of New York, Institute for Ultrafast Spectroscopy and Lasers, Physics Department, MR419,
160 Convent Avenue, New York, New York 10031

Abstract. We present an overview and history of terahertz (THz) sources for readers of the biomedical and optical community for applications in physics, biology, chemistry, medicine, imaging, and spectroscopy. THz low-frequency vibrational modes are involved in many biological, chemical, and solid state physical processes.
 [DOI: 10.1117/1.3554742]

Keywords: terahertz sources; time domain terahertz spectroscopy; pumps; probes.

Paper 10449VRR received Aug. 10, 2010; revised manuscript received Jan. 19, 2011; accepted for publication Jan. 25, 2011; published online Mar. 22, 2011.

1 Introduction

One of the most exciting areas today to explore scientific and engineering phenomena lies in the terahertz (THz) spectral region. THz radiation are electromagnetic waves situated between the infrared and microwave regions of the spectrum. The THz frequency range is defined as the region from 0.1 to 30 THz. The active investigations of the terahertz spectral region did not start until two decades ago with the advent of ultrafast femtosecond lasers.

The T-rays in various energy units are displayed in Table 1**,** summaring

1 THz ⇔ 33.3 cm^{-1} ⇔ 300 μm ⇔ 4.1 meV ⇔50 K.

A large number of materials are transparent in the T-spectral range. T-waves can pass through opaque dry media that are opaque to visible and near-infrared waves. T-waves are strongly absorbed by waterlike media (see Fig. 1). Many important molecular low-frequency vibrational modes can be measured in the terahertz region from rocking, torsional, and conformational molecular changes. In the past, the lack of investigation of materials with T-rays was due to the lack of convenient and high-power THz sources. This frequency region was traditionally named the "far-infrared" and the most common far-infrared sources used from the 1960s up to now have been Black Body Radiation Sources, such as a Globar source. A Globar source is a resistively heated silicon carbide rod that operates at high temperature. A Globar source emits over an extremely wide spectral region (into the THz region) but with a very weak output power of the order of picowatts. Globars are used to light gas ovens. Mercury arc lamps generate electromagnetic waves in the THz region like a Globar source but with more powerful radiation. A commercially available 75-W Hg arc lamp (available from Sciencetech, Inc.) generates broadband continuous THz radiation in the 5–100 cm^{-1} spectral region. This lamp is ~8× more powerful than a Globar source in the 5–30 cm^{-1} region, and about 2–3x more powerful in the 30–100 cm^{-1} region.

At the end of the 1960s and in the early 1970s, the pioneering works by Faries et al.,[1] Morris and Shen,[2] Yang et al.,[3] and Yajima et al.[4] first reported on tunable far-infrared radiation by optical difference-frequency mixing in nonlinear crystals. These works have laid the foundation and were used for a decade and initiated the difference-frequency generation (DFG), parametric amplification, and optical rectification methods.

The THz region became more attractive for investigation owing to the appearance of new methods for generating T-rays based on picosecond and femtosecond laser pulses. Many different sources can now generate T-rays either in short-pulse mode or continuous wave (cw) mode with output power ranging from the nanowatt level up to 10 W (see Fig. 2).

Today, the two most commonly used methods of T-ray generation are based on photoconductive antenna (PCA) and optical rectification (OR). These two methods are used widely in the field of T-ray spectroscopy. Pioneering works on the PCA effect were reported[3–7] in the microwave (gigahertz) range first by Mourou et al.,[5] and later, this effect was further expanded into the THz region by research groups led by Auston[6,7] at Bell Labs and Grischkowsky[8,9] at IBM Watson Research Center. The OR method was first used and described in greater detail[10,11] by Zhang, who really pushed this method forward into worldwide use. It is important to note that Zhang introduced this method to Alfano's group at CCNY in the early 2000s and to many others. He stimulated other researchers in the world to pursue T-spectroscopy.

The T-sources based on both of these methods are now commercial products offered by several companies. Among them are Picometrix Inc. (Michigan), Zomega Terahertz Corporation (New York), TeraView Limited, Nikon Corporation, Toptica Photonics, Hamamatsu Photonics, T-Ray Science Inc., and others. The output power of these sources is from tens of nanowatt to tens of microwatt ranges. Today, other methods can even produce stronger T-ray radiation, such as DFGs, quantum cascade lasers (QCL), and p-Ge lasers.

This paper highlights the different types of THz sources for the benefit of the biomedical optical community that are used today for science and engineering applications. A history is briefly given on the important icon in the field. In biology and medicine, low-frequency T-sources are widely used in the range 1–3.5 THz for investigations of conformational

Address all correspondence to Robert R. Alfano, City College of New York, Institute for Ultrafast Spectroscopy and Lasers, Physics Department, 160 Convent Ave., New York, New York 10031. Tel: 212–650–5533; Fax: 212–650–5530; E-mail: ralfano@sci.ccny.cuny.edu

1083-3668/2011/16(3)/033001/9/$25.00 © 2011 SPIE

Table 1 THz rays defined in different units.

Frequency $\upsilon = c/\lambda$ (THz)	Wavenumber $\upsilon = 1/\lambda$ (cm^{-1})	Wavelength $\lambda = c/\upsilon$ (μm)	Energy $E = h\nu$ (meV)	Equivalent Temperature $T = E/k$ (K)
0.1	3.33	3000	0.41	5
1.0	33.3	300	4.1	50
10.0	333	30	41	500
30.0	999	10	123	1500

Where: c-speed of light, h-Planck constant, and k-Boltzmann constant.

molecular changes, chemical reactions in myoglobin (1.515 THz), hemoglobin (1.17 THz), primary events in vision (1.8 THz), and many others. THz spectroscopy has become as common as Raman spectroscopy. This paper covers most of the current THz sources we believe represent the best methods, but not the entire field. The use in medicine is limited to deep tissue because of the large absorption by water.

2 Optically Pumped Short-Pulse THz Sources

As stated above, the most commonly used methods for T-ray generation are based on ultrashort optical laser pulses. These are the PCA and OR methods. Both of these methods are based on optically exciting a medium. The parameters of the excited T-rays depend on the nonlinear medium, pump laser pulse duration and pulse energy.

The commonly used pulse laser for exciting the nonlinear crystals is a femtosecond Ti-sapphire laser at 800 nm wavelength with a pulse duration <100 fs. The Ti-sapphire oscillator is pumped by a Nd:YAG laser or by a Nd:YVO4 laser. The laser system can generate ultrashort pulses with pulse duration of <100 fs, average power ~1 W at a repetition frequency of 250 kHz. This system is expensive, which leads us to search for smaller, less costly femtosecond lasers. A less expensive compact fiber-laser system based on the IMRA Femtolite H-100-laser with a pulse duration of 150 fs, average power ~100 mW, and repetition frequency of 75 MHz at 810 nm wavelength (second harmonic of radiation) can be used for T-spectroscopic measurements. The latest IMRA D-400 and D-1000 lasers offer even more powerful femtosecond pulses and can excite even higher T-ray power.

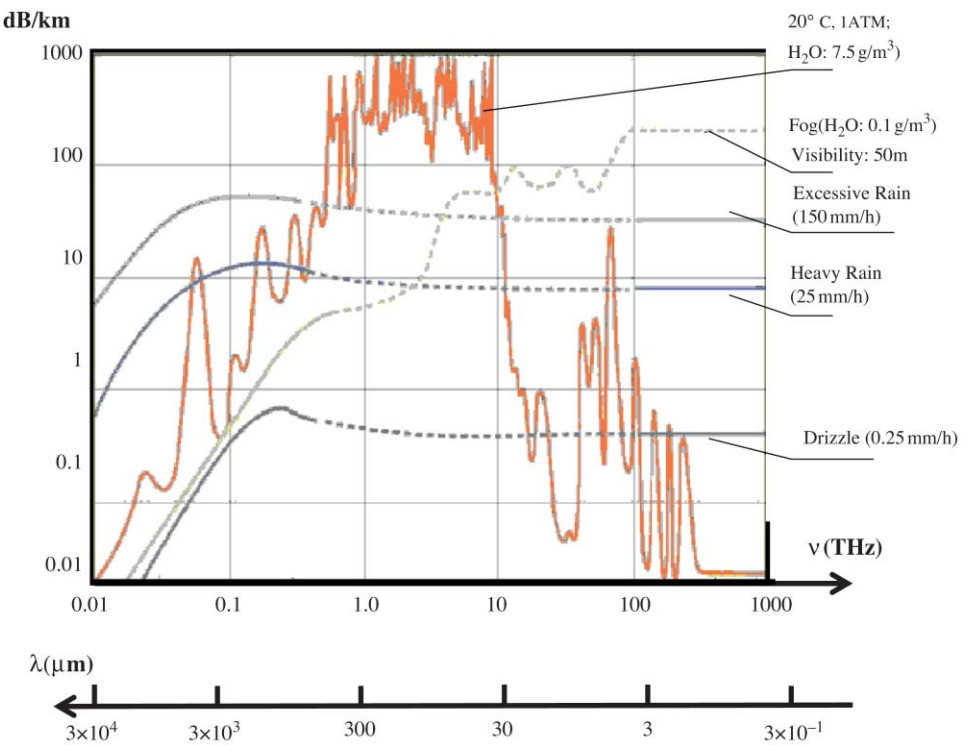

Fig. 1 Electromagnetic wave attenuation by atmospheric H_2O versus frequency in the range 10^{10}–10^{15} Hz.

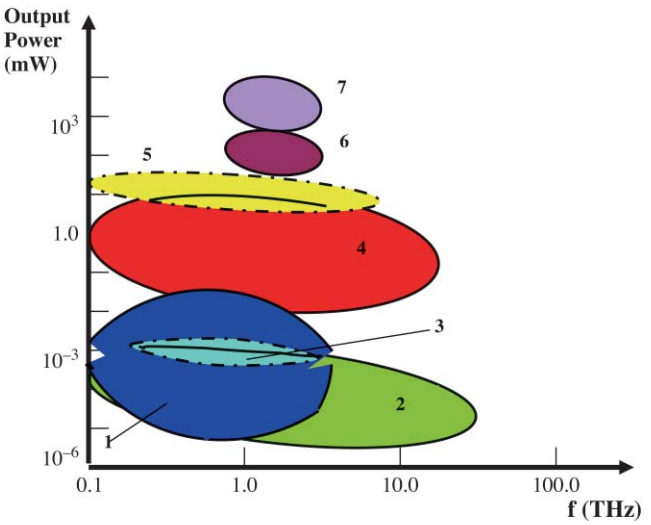

Fig. 2 Output average power ranges of THz-sources depending on frequency range.

2.1 *Photoconductive Antenna*

One of the first and oldest methods of producing T-rays is based on PCAs by Mourou et al.[5] and Auston et al.[6,7] This method is commonly called the "Auston Switch," which is based on carriers photoexcited into the conduction band of a semiconductor by ultrashort laser pulses. The photon energy of the laser pulse must be larger than the bandgap of the semiconductor. In this case, the laser pulse excites electron-hole pairs in the semiconductor to break down an electronic switch, which shorts out an applied bias voltage to produce high-voltage pulses and THz radiation.

The active transmitter is a split antenna consisting of two small metal strips deposited lithographically on a semiconductor crystal wafer (silicon). The strips are under a bias voltage of around 10–20 V. The split-antenna gap is around 10–30 μm. The pump laser beam is focused into the point of the split gap. The carriers are accelerated by the bias voltage (field of ~10,000 V/cm) and create wideband THz pulses. The semiconductor physical parameters and the laser ultrashort pulse intensity and duration define the intensity and bandwidth of the THz radiation.

A number of semiconductor crystals are used for the sources: Si, GaAs, InAs, InP, and ZnTe. PCA sources can emit THz radiation in the bandwidth 0.1–4 THz,[9] with an average radiation power of up to 40 μW.[12] A record value of average radiation power of 100 μW was reported,[13] and a record value of signal-to-noise (S/N) ratio of around 10,000/1 was achieved. Typical values of average radiation power of PCA sources are in the wide range from 10 nW to several microwatts depending on the infrared pump power and dc bias voltage. Typical values of S/N ratio obtained in experiments are in the range from 2000/1 to 5000/1.

Today, PCA T-ray systems are commercially available products which provide T-rays in the spectral range 0.1–3 THz with average output power radiation of up to several tens of microwatts.[14]

2.2 *Optical Rectification*

OR is the most common and easier method for T-ray generation. The method does not require antenna fabrication. It is based on the inverse electro-optical second-order effect in a nonlinear crystal,[10,11] similar in operation to the quadratic optical Kerr effect. In this case, the energy of femtosecond pulses from a pump laser directly gives rise to T-rays, without applying any bias voltage to the semiconductor crystal. The OR method uses the electric field of the laser femtosecond pulses themselves. The OR mechanism is similar to the frequency-mixing and second-harmonic generation process in a nonlinear medium $\chi^{(2)}$. When broadband laser radiation with intensity $I(t,\omega)$ and with any two frequencies ω_1 and ω_2 (in the pulse spectrum) interacts with the nonlinear medium, the result is an induced polarization $P(t,\omega)$ at the sum-frequency ($\omega_1 + \omega_2$) and difference-frequency ($\omega_1 - \omega_2$) components of the electromagnetic field $E(t, \omega)$,

$$E(t, \omega_1 \pm \omega_2) \propto \frac{\partial^2 P(t, \omega)}{\partial t^2} = \chi^{(2)} \frac{\partial^2 I(t, \omega)}{\partial t^2}. \quad (1)$$

The sum-frequency component of $E(t, \omega_1 \pm \omega_2)$ corresponds to the second-harmonic process and the difference-frequency component corresponds to the "dc"-pulse for the case $\omega_1 = \omega_2$. This dc-pulse $\{E(t)^2 \sim (\chi^{(2)})^2\}$ is similar to the envelope of the frequency beating in broadband femtosecond pump laser radiation. Femtosecond optical pulses have a bandwidth of around a few THz and the Fourier-transform (FT) spectrum of $E(\omega) = \mathrm{FT}\{E(t)\}$ covers the THz region from 0.1 to ~10 THz. The resulting THz rays $[E_{\mathrm{Thz}}(t)]$ usually cover the frequency region from 0.1 to ~5 THz. The shape and bandwidth of the T-ray pulses correspond to the envelope of the optical pulses, which depends on the optical pulse duration and $\chi^{(2)}$ nonlinearity of the semiconductor crystal.

There are a number of semiconductor crystals used in optical rectification sources, such as ZnTe, $LiNbO_3$, GaAs, and GaSe. The ZnTe crystal is most commonly used due to the phase-matching criterion of the THz frequency band and optical frequency. The other materials were also selected based on the same phase-matching criterion, where the THz wave phase velocity in the crystal and the group velocity of the optical pulse are phase matched.

The phase-matching condition is important to generate intense THz radiation by the OR method. When broadband pulse laser radiation at frequencies $\omega_1 = \omega_2$ and $\omega_1 = \omega + \Omega$ interacts with a nonlinear medium where Ω is in the THz frequency range, the induced dielectric polarization of the medium at THz frequencies becomes

$$P_{\mathrm{THz}}(t, \omega, \omega + \Omega) = \chi^{(2)} E(\omega) E^*(\omega + \Omega). \quad (2)$$

The efficiency of the frequency-mixing and OR processes grows significantly at the phase-matching condition[15] given by

$$\Delta k = k(\omega + \Omega) - k(\omega) - k(\Omega), \quad (3)$$

where $k = \omega/c$ is the wavevector, $c = n_g \upsilon_g$ is the speed of light, υ_g is the group velocity of light, and n_g is the group velocity refractive index of medium.

The propagation constant $k(\omega + \Omega)$ can be expanded into a series around ω,

$$k(\omega + \Omega) = k(\omega) + \left.\frac{\partial k}{\partial \omega}\right|_{\omega} \Omega + \left.\frac{\partial^2 k}{2\partial \omega^2}\right|_{\omega} \Omega^2 + \cdots . \quad (4)$$

Combining Eqs. (3) and (4) and neglecting second-order and higher order terms,

$$\Delta k = \left.\frac{\partial k}{\partial \omega}\right|_{\omega} \Omega - k(\Omega). \quad (5)$$

Setting the phase-matching condition $\Delta k = 0$ [Eq. (3)], we obtain

$$\left.\frac{\partial k}{\partial \omega}\right|_{\omega} \Omega = k(\Omega). \quad (6)$$

From

$$k(\Omega) = \Omega \frac{n(\Omega)}{c} \quad \text{and} \quad \left.\frac{\partial k}{\partial \omega}\right|_{\omega} \Omega = \frac{n_g(\omega)}{c}\Omega, \quad (7)$$

we obtain the result that with the phase-matching condition for an incident pulse laser wave (ω) and an output THz wave (Ω), the group velocity refractive index at $\omega[n_g(\omega)]$ is equal to the THz wave refractive index n (Ω). The condition is as follows:

$$n_g(\omega) = n(\Omega). \quad (8)$$

It should be noted that the main disadvantage of this method of THz generation is the relatively low conversion efficiency ($\sim 10^{-6}$) of optical pulse energy to THz pulse energy. The power of these T-ray sources lies in the range from nanowatt up to submicrowatt level. However, a high S/N ratio (up to 5000/1) and extremely wide bandwidth (up to 50 THz) can be achieved in experiments with GaAs and GaSe.[11,16] THz pulse generation has been reported over a wide spectral range from 5 to 41 THz and a THz pulse duration as short as 50 fs was obtained from a thin (90 μm thick) GaSe crystal by phase-matched optical rectification.[17]

THz radiation of ultrashort pulses generated by the OR method are continuously emitted over a wide interval extending smoothly into the far-infrared region. Typical average power levels of T-sources lie in the microwatt range. These kinds of T-ray sources are widely used in time-domain terahertz spectroscopy (TDTS) of materials. TDTS and pump/probe setups based on OR sources are widely used to investigate the molecular spectra of a number of materials, including water, semiconductors, chemical, vapors, proteins, and bacteria.[11,16,18–26]

3 Frequency Downconversion

Far-infrared generation by frequency downconversion was obtained in 1969 through the 1980s using photomixing and frequency mixing of laser frequencies in nonlinear crystals[1–4,7,8,28,29] and open antenna structures.[27]

3.1 *CO_2-Laser Frequency Mixing*

T-rays can be generated using one or two cw CO_2 gas lasers by frequency mixing. This method was introduced first in 1984.[30] DFG was obtained by mixing two laser frequencies (with the frequency difference falling in the THz region) in an open antenna structure based on a metal-insulator-metal [(MIM), W-Ni] point contact mixer. This method gave rise to tunable cw THz emission up to 6 THz because of the abundance (several thousands) of CO_2 gas laser lines in the range of 9–11 μm and the uniquely fast response (up to 260 THz) of the MIM diode. A logical sequel to this method was to use two frequency-stabilized CO_2 lasers and one frequency-tuned microwave generator for third-order frequency mixing in the same MIM diode and later using a commercially available Schottky diode. By downconversion of two CO_2 lasers (second-order mixing), it is possible to generate a T-ray power of around 1 μW. These THz sources can generate narrowband ($\sim$1 MHz and less) cw radiation in discrete parts of the 6-THz range. The disadvantage of the method is the relatively small spectral tunability and the small downconversion efficiency ($\sim 10^{-6}$) with the low level of output power that lies in the microwatt range.

3.2 *Difference-Frequency Generation in Nonlinear Crystals*

Optical laser frequency mixing in second-order [$\chi^{(2)}$] nonlinear materials was first used successfully for far-infrared generation by optical beat-frequency by Faries et al.,[1] Morris and Shen,[2] Yang et al.,[3] and by Yajima et al.[4] In the first case,[1–3] $LiNbO_3$ and quartz were used as mixing crystals for DFG between two temperature-tuned ruby lasers. In this case, narrowband tunable radiation was generated in the range of 1.2–8.1 cm^{-1} with a peak output power of $\sim$1 mW. In the second case,[4] $LiNbO_3$, ZnTe, ZnSe, CdS, and quartz were used as mixing crystals for DFG between two modes of a mode-locked Nd:glass laser. Generation of broadband T-radiation in the range of 1–20 cm^{-1} was achieved.[4]

The method of T-ray generation by parametric frequency down-conversion was first demonstrated by Campillo and Shapiro in 1979.[28,29] In that work, a mode-locked Nd:YAG laser (1.064 μm) was used as a pump source for an optical parametric oscillator based on two-step parametric amplification in two $LiNbO_3$ crystals. The parametric oscillator emitted tunable infrared radiation in the range 1.92–2.38 μm, which was directed into a CdSe crystal mixer and excited tunable DFG in the range of 14.8–18.5 μm. The pump (1.064 μm) energy was $\sim$10 mJ, the parametric oscillator (2 μm) emitted $\sim$0.5 mJ, and DFG T-ray energy was $\sim$2 μJ in a spectral range near 16 μm.

Cw and pulsed tunable diode-lasers in the near-infrared range and lasers based on semiconductors, such as GaAs, can be used for DFG creation.[7,8] Pulsed or cw sources can be used for T-ray generation by the photomixing process. In this case, two collinear laser beams with different frequencies are mixed in a mixer to create a cw T-source by the process of downconversion. The created T-rays are collected and integrated into a mixer-antenna structure and directed into space by an off-axis parabolic mirror. The advantages of this technique are that continuously tunable T-rays over the frequency range from 0.1 to 3 THz and spectral resolutions of the order of 1 MHz can be achieved.

Pulsed lasers create DFG sources based on a mixing process similar to the optical rectification process in the common case of a frequency ω_1 not equal to the frequency ω_2. Two tunable single-color diode-laser beams or one two-color diode-laser beam are focused into a semiconductor antenna structure

and produce a photocurrent in the antenna structure, modulated at a beat frequency that falls in the THz region. The beat signal induces electromagnetic waves in the semiconductor antenna, which works as a T-ray emitter.

Many nonlinear materials, such as semiconductor crystals and organic polymers, have been used as frequency mixers. Work has been reported[31] on DFG by frequency mixing of two infrared fiber-laser beams in the GaSe semiconductor crystal to produce far-infrared radiation. Both of the pump fiber lasers had summing output average power of ~900 mW and produced 0.43 μW average power in the 1.5 THz range.

Researchers[32,33] have introduced new effective organic nonlinear materials that provided wideband coherent THz radiation. In one work,[32] a double-crystal KTiOPO4 (KTP) was used in an optical parametric oscillator pumped by a frequency-doubled (532-nm) Nd:YAG pulsed laser (7-ns pulse duration). The double-crystal dual-color (750–950 nm) KTP laser pumps a nonlinear organic crystal BNA, which generates a difference frequency in the range of 0.1–20 THz. The system has good efficiency of frequency conversion. The pump laser's (532–850 nm) conversion efficiency is ~13%, and the infrared-to-THz (0.85–214 μm) conversion efficiency is ~0.0004%. The maximum THz-pulse energy achieved in this experiment is ~140 pJ/pulse in the 1 THz range and ~200 pJ/pulse in the 6 and 11.6 THz ranges, which corresponds to ~20–30 mW of pulse output power.

In another work,[34] a DFG source based on a Dendrimer (polymeric nanomaterial) film waveguide emits T-rays in the 0.5-THz range, with an average power of ~60 μW, which corresponds to a conversion efficiency of $\sim 10^{-4}$.

4 Optically Pumped THz Lasers

Optically pumped THz lasers can operate from molecular rotational transitions of gases like CH_3OH, CH_3OD, CH_3F, CF_4, and others. Single-line high-power CO_2 lasers in the range of 9–11 μm are used for pumping the molecular transitions and exciting laser action in the 0.1–8 THz range. The most popular THz laser is the CH_3OH laser ($\lambda_{THz} = 118.83$ μm, $\lambda_{pump} = 9.6$ μm). It has achieved a very high ($\sim 10^{-2}$–10^{-3}) infrared-to-THz wave conversion.[35,36] The advantages of optically pumped lasers are the very narrow emission lines (1 MHz and less), which produce the very high spectral brightness of these THz sources and high output power. The power level of this kind of lasers lies in the range of several tens of milliwatts. Some commercially available CH_3OH lasers emit cw coherent radiation with an output power up to 100 mW. The disadvantage of these sources is the relatively small spectral tunability (~2 cm^{-1}) because the laser action is connected to the discrete frequencies of molecular transitions.

5 Quantum Cascade Laser

One of the major advances in THz sources is using coupled quantum wells, as introduced by Capasso's group[37] in 2-D structures. The QCL laser was demonstrated first in the middle-infrared region (~70 THz) in 1994.[38] More recently the QCL in the THz range (4.4 THz) was introduced in 2002.[39] This laser emits high-power (tens of milliwatts) THz radiation at discrete frequencies from electronic intersubband transitions in semiconductor heterostructures. The active semiconductor structure is realized based on a multiple quantum-well (QW) heterostructure in a GaAs/AlGaAs sandwich. The laser consists of coupled QWs constructed by nanometer-thick layers of GaAs sandwiched between potential barriers of AlGaAs. The quantum cascade consists of a repeating structure in which each repeat unit is made up of an injector and active region. In the active region, a population inversion exists and electron transitions to a lower energy level occur, emitting photons at a specific wavelength. The electrons then tunnel between quantum wells, and the injector region couples them to the higher energy level in the active region of the subsequent repeat unit. The main problem in the development of THz QCLs is caused by the long wavelength of the THz radiation, buildup of electrons in lower levels, and a phonon bottleneck. The former effect results in a very large optical mode, which results in poor coupling between the optical field and the gain medium, and high optical losses owing to free electron absorption in the medium. The optical losses scale as the square of the wavelength. Initial breakthrough developments have taken place in both the QW gain medium and in a waveguide structure. The resonant-phonon scheme takes advantage of subpicosecond electron-longitudinal-optical (LO) photon scattering to selectively depopulate the lower energy level, together with using a metal-metal ridge waveguide, similar in form to a microstrip transmission line.

The first operational QCLs in the THz range required cooling to very low temperature (down to 50 K) for laser action and operated in pulsed mode only with an average output power of several milliwatts. The advantages of QWs are the provision of high-confinement and low-loss cavity for THz QCLs.[40,41] At present,[42] QCLs provide T-rays in the region of 0.84–5.0 THz with very high pulsed average output power (250 mW) at low operating temperature of ~169 K and very high CW output power (130 mW) at an operating temperature of ~117 K.

The advantage of THz QCLs is the high output power (hundreds of milliwatts) in both pulsed and cw modes. The need for a cryostat for low-temperature operation is the main disadvantage of QCLs. Recently, Capasso's group[43,44] and Amann's group[45] reported on high-temperature operation (up to 420 K) of QCLs in the midinfrared range of 4.5–9 μm. In these cases, QCLs generate midinfrared radiation in both pulsed and cw modes with an output power in the 0.3–1.0 W range. Work is needed to raise the operating temperature of THz QCLs to values accessible by thermoelectric coolers (~240 K) or even better, up to room temperature. For this purpose, it is necessary to overcome the two main processes of degradation of population inversion in THz QCLs at higher temperatures: thermal backfilling of the lower laser level and thermally activated LO-phonon scattering of the upper level. The first process is caused by electrons from the heavily populated injector and occurs either by thermal excitation or by reabsorption of LO phonons (hot phonon effect). The second degradation process takes place as electrons in the upper subband acquire sufficient kinetic energy to emit an LO phonon and relax to the lower subband.[42]

An alternative way to produce T-rays using QCLs was introduced in Ref. 46 by combining the recent advantages of the midinfrared QCLs and DFGs. This source is based on the

dual-wavelength QCL ($\lambda_1 = 7.6\ \mu$m, $\lambda_2 = 8.7\ \mu$m), which produces difference-frequency THz-radiation at a wavelength $\lambda_{THz} = 60\ \mu$m. This THz-QCL/DFG source emits an output powerof ~60 nW in cw mode and operates at a temperature of 80 K.

6 P-Germanium (p-Ge) THz Laser

The most powerful T-ray source of all that produces an output power of several watts is the p-Ge laser.[47,48] The high output power of the p-Ge laser is very attractive for use in THz imaging, remote sensing and engineering applications. The p-Ge laser is based on hole intervalence band transitions in germanium semiconductor. The population inversion of the hole levels for laser action is achieved from direct optical transitions between the Landau levels of light holes and heavy holes of subbands of the germanium valence band at low temperature. The operation of the p-Ge laser requires high electric (E) and magnetic (B) fields. The trajectory of a hole moving in the presence of E and B fields is a cyclotron trajectory. Under some temperature and field conditions, the holes are accelerated without scattering until they reach the optical phonon energy. Because of the higher effective mass of heavy holes ($M_{hh}/M_{lh} = 8$), heavy holes reach the optical phonon energy at a smaller E/B ratio than light holes. In a certain range of the E/B ratio (typically, 0.7–2.0 kV cm^{-1}/1–2 T), the heavy holes reach the optical phonon energy level and get scattered into the light hole band, creating a population inversion and optical photon emission via lasing in the THz region.

The Ge-crystal can be doped with hydrogenic acceptors like gallium, aluminum, and thallium, or with nonhydrogenic acceptors such as beryllium, zinc, and copper for better operation. The doping concentration lies in the range of 10^{14}–10^{15} cm^{-3}, depending on the acceptors. Be-doped Ge-crystal was found to be a more efficient active material for this kind of T-laser. The working temperature of the crystal is in the range of 40–80 K. The pulsed electric field is around 1–2 kV cm^{-1} and the permanent magnetic field is around 1–2 T. The magnetic field can be applied along the optical wave direction or perpendicular to the wave direction. It was revealed that the perpendicular case is more efficient for laser action and leads to a more compact laser design. The crystallographic orientation with respect to electric and magnetic fields also influences laser operation. The ⟨110⟩ crystal orientation with the magnetic field parallel to the ⟨110⟩ axis direction is favorable for optimum laser action.

The recent development of a high-power Be-doped Ge THz laser is described in Refs. 47–50. The laser crystal with a doping concentration of 1.1×10^{14} cm^{-3} and size of $30 \times 4 \times 3$ mm^3 was placed between cooling copper bars inside crossed E and B fields. The pulse length, frequency and high-voltage value of the E-field can be varied in the range 1–2 kV cm^{-1} using commercial and homemade electric generators. The magnetic field (1.2 T) was created by two small permanent magnets so that the B-field was perpendicular to the E-field and to the optical axis of the laser. The laser emits pulses up to 32 μs at repetition rates of up to 45 kHz. The output average power is several watts. By tuning the E and B fields, the laser operates in the frequency range of 1–4 THz.

Recent papers report on increased crystal volume, resonator design, and applied fields to generate an output power from a p-Ge-laser of up to 10 W.[49] The main disadvantages of this kind of laser are the operational requirements for a cooling dewar, high magnetic, and pulsed electric fields. The unique parameters of the p-Ge-laser allow coherent radiation to be produced over a wide THz range with wide continuous spectral tunability and very high output power in the range of several watts making this kind of THz laser very attractive for spectroscopic and imaging applications.[50–53]

7 T-Sources in Typical THz Spectroscopy Setups

PCA and OR sources are the most commonly used sources in TDTS spectroscopy systems. In this section, a brief review is given on these two methods in a pump-probe T-ray spectroscopy setup.

7.1 *T-Ray Spectroscopy Setup Based on a Photoconductive Antenna Source*

A typical TDTS transmission spectroscopy setup based on a PCA source is shown schematically in Fig. 3(a). The output beam of pumped infrared (~800 nm) radiation from a femtosecond Ti-sapphire laser is divided by a beam splitter into two parts, so that the higher portion of the pump power goes into the transmitter arm and the lower portion goes into the receiver arm. The optical lengths of both arms are adjusted to be approximately equal (path difference is defined by a selected value of time delay) by using a variable delay line. The infrared pump laser beam is focused by the lens into a point in the split gap of the transmitter antenna. A pulse of THz radiation is generated by the transmitter at the instant that the antenna is illuminated by the pump femtosecond pulse. The THz pulse emitted by the transmitter is collimated by the off-axis parabolic mirror, which produces a parallel THz beam. A sample is located in the THz beam between two parabolic mirrors. After passing through a sample, the THz beam is collected by a second parabolic mirror and focused into a point in the split gap of the receiver antenna.

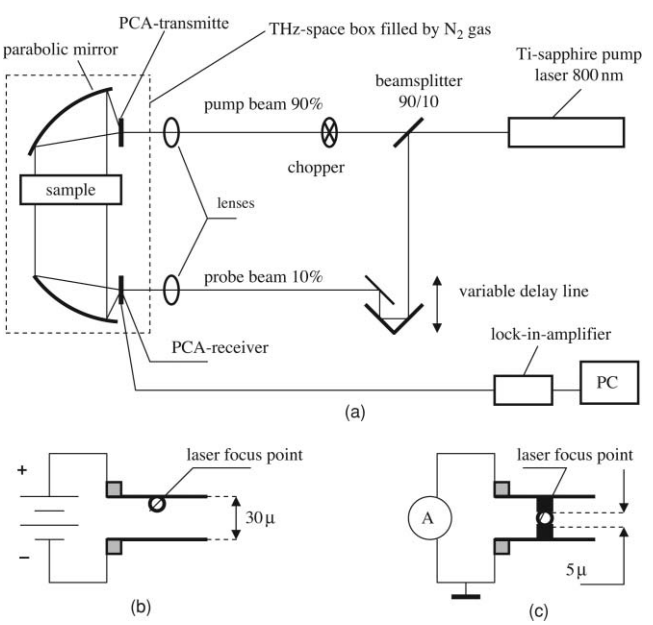

Fig. 3 (a) Schematic diagram of TDTS spectrometer based on PCA source, (b) schematic diagram of the PCA transmitter, and (c) schematic diagram of the PCA receiver.

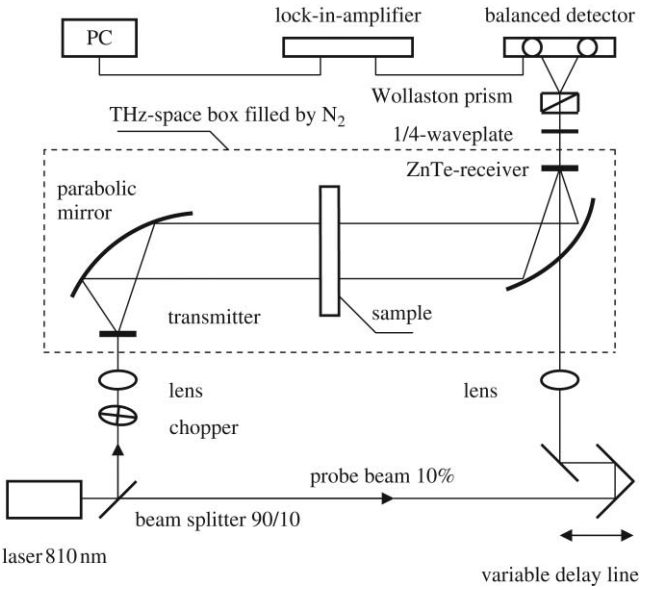

Fig. 4 Schematic diagram of TDTS spectrometer based on OR source (pump/probe setup).

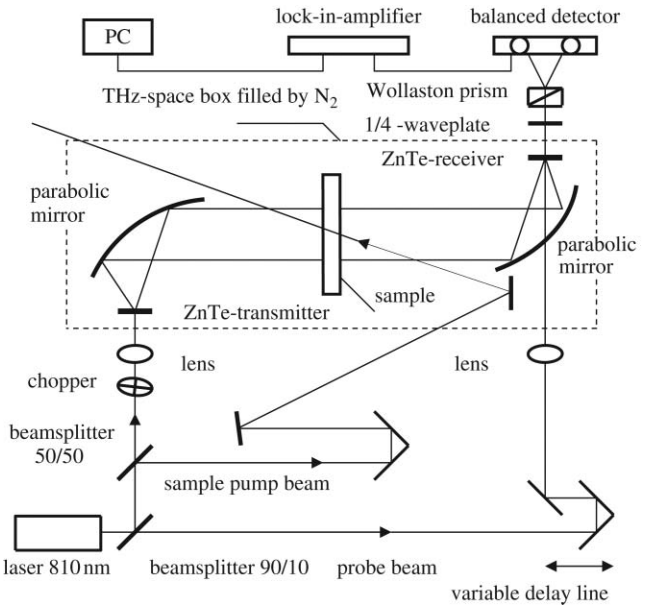

Fig. 5 Schematic diagram of TDTS spectrometer based on OR source (pump/pump/probe setup).

The receiver antenna is gated synchronously with the THz pulse and infrared femtosecond probe pulse, so that the current flow at the receiver maps out the time-dependent electric field of the THz pulse as the variable delay line is adjusted. The transmitter and receiver split antennas consist of two small metal strips deposited lithographically on a semiconductor crystal wafer. The strip-line length is ~1.6 cm, and the split-antenna gap is around 10–30 μm. The strips are at a dc bias voltage around 5–20 V. The infrared pump and probe laser beams are focused by lenses into points on the split gap of both (transmitter and receiver) antennas. Schematic diagrams of the transmitter and receiver PCAs are shown in Figs. 3(b) and 3(c). A laser focus point in a transmitter PCA [Fig. 3(b)] is shifted close to the anode strip because such a focal position is more effective for THz generation.[16]

The receiver antenna structure is similar to the transmitter structure, except that the antenna has a 3–5 μm gap size in the center of a transmission stripline [Fig. 3(c)]. A laser focus point is displaced in the center of structure into ~5μm gap between strip lines in a receiver PCA [Fig. 3(b)].[16] Another distinction is the absence of an applied dc bias voltage to the gap. The transient THz pulse field itself provides the bias voltage (autobias effect). The time delay between the pump laser and T-ray pulses is varied, and an output *E*-signal from the detector is plotted on the PC-controlled display as a synchronized time-delayed pulse curve. The dynamic range achieved is 10,000/1. These PCAs are from Hamamatsu Photonics and T-Ray Science, Inc.

7.2 *T-Ray Spectroscopy Setup Based on OR Source*

The most commonly used THz source in the field of TDS is based on an OR source. A schematic diagram of the CCNY/IUSL TDTS transmission spectroscopy setup based on an OR source is shown in Fig. 4. The output beam of the pump infrared (~800 nm) radiation from a femtosecond Ti-sapphire laser (our option is to use an IMRA F-100 fiber laser) is divided into two (in the ratio ~90/10 for the probe setup), or three (in the ratio ~45/45/10 for the doubling pump/pump/probe setup as shown in Fig. 5) optical arms. The optical lengths of the arms are adjusted to be approximately equal (the path difference is defined by a selected value of time delay) by using a variable delay line. The THz pulse is generated by the transmitter crystal, which is based on a ZnTe semiconductor. The receiver is the same as the transmitter ZnTe(110) crystal plate with the same thickness (usually around 1 mm). Both crystals are located at the focal points of offset parabolic mirrors. One of the parabolic mirrors has a small hole in its center for transmission and collinear adjustment of the probing infrared beam to the THz beam. The sample is placed in the parallel THz beam between the two parabolic mirrors. The polarization of the infrared pump/probe beams and THz beam are parallel to the ZnTe crystal (110) direction.

The OR source is based on the quadratic optical Kerr effect (investigated by Ho and Alfano[54] for electro-optical detection of a probed THz signal). When the broadband THz pulse, emitted by the transmitter crystal, leaves the sample and passes through the receiver crystal, the birefringence of the infrared probing pulse, which passes through the receiver crystal at this instant, is modulated synchronously by varying the intensity of the electric field of the transmitting THz pulse. This change of electric-field component of the probing infrared beam is measured with a λ/4–wave plate, a Wollaston prism, and a balanced detector connected to a lock-in amplifier. A beam chopper modulates the THz beam or the infrared beam, which pumps the transmitter, for sensitive synchronous detection. The time delay between the infrared pump and T-ray pulses is varied, and the output *E*-signal from the balanced-detector is plotted on the PC-controlled display as a synchronized time-delayed pulse curve. The dynamic range achieved is 5000/1 over the range of 0.2–2.4 THz.

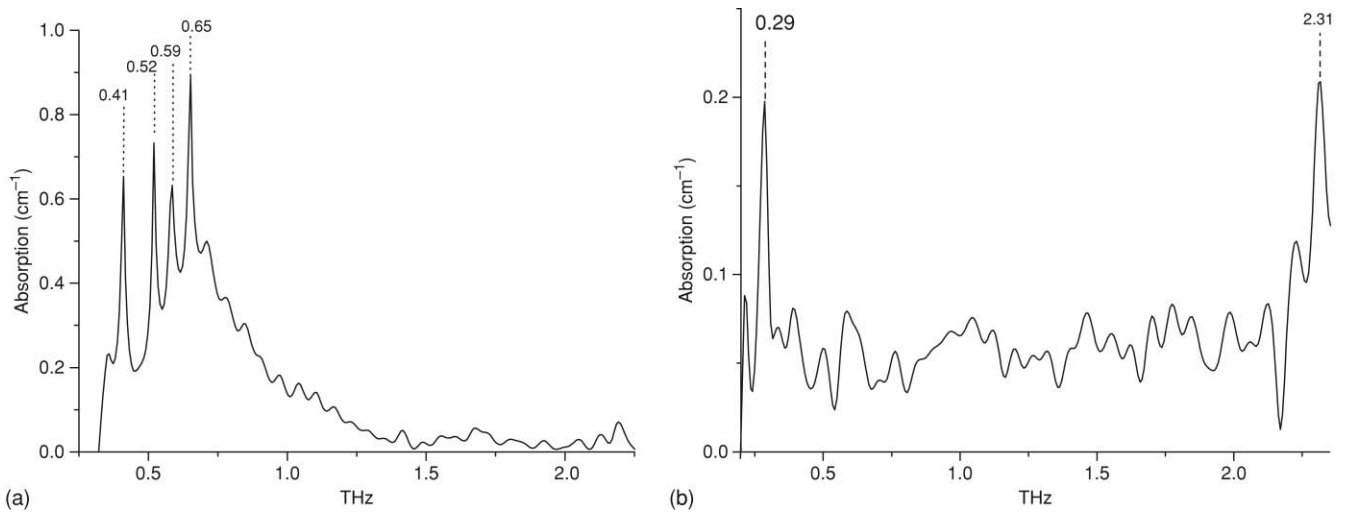

Fig. 6 (a) THz spectra for acetone (C_3H_6O) vapor and (b) THz spectra for toluene (C_7H_8) vapor.

8 Some Examples of IUSL THz-Spectroscopy Measurements

The CCNY/IUSL has been engaged in THz-spectroscopy investigations since the early 2000s, headed first by B. Yu and now by P. Shumyatsky. The research has focused on optical and semiconductor materials, biomolecules, liquids, vapors, and gases. The THz-time-domain–time-resolved spectroscopy method has been shown to be a powerful tool for materials research.

The following materials have been investigated: Tryptophan,[18] water (liquid H_2O and D_2O, vapors of both of them),[19–21] liquid CS_2,[22] CH_3OH and its isotopes (CH_3OD and CD_3OD) gases,[23] Freon-11 (CCl_3F, CFC-11),[24] Bacillus subtilis spores and DPA,[25] semiconductor crystals GaSe,[26] and GaAs.[27] The THz-absorption spectra, refractive indices, dielectric properties, and phonon relaxation times were measured by the TDTS pump-probe method (see setup shown in Figs. 4 and 5) in the 0.2–2.4 THz range. Figure 6 shows the THz spectra of acetone and toluene vapors.

The typical thickness of measured solid and liquid materials was in the range from 0.1 to 2 mm. A new technique using a waveguide sample holder in TDTS has been recently developed to measure smaller quantities of materials and particles with better spectral resolution of the absorption spectra.[55] This technique should lead to improved accuracy in determining the "spectral fingerprints" for identification purposes and can be used for Homeland Security applications, and THz "photonic nose" for vapors detection around a body.

9 Conclusion

This paper presents most of the operational THz sources in the spectral range from 0.1 to 30 THz. The paper does not elaborate on all THz sources. These THz sources are attractive for science, medicine, imaging, and engineering applications.

Acknowledgments

This work is supported in part by internal IUSL funds, DoD, NASA, and NYSTAR's Photonic Student Training program for high school and undergraduate students.

References

1. W. Faries, K. A. Gehring, P. L. Richards, and Y. R. Shen, "Tunable far-infrared radiation generated from difference frequency between two ruby lasers," *Phys.Rev.* **180**(2), 363–365 (1969).
2. J. R. Morris and Y. R. Shen, "Far-infrared generation by picosecond pulses in electro-optical materials," *Opt. Commun.* **3**(2), 81–84 (1971).
3. K. H. Yang, P. L. Richards, and Y. R. Shen, "Generation of far-infrared radiation by picosecond light pulses in $LiNbO_3$," *Appl. Phys. Lett.* **19**(9), 320–323 (1971).
4. T. Yajima and N. Takeuchi, "Far-infrared difference-frequency generation by picosecond laser pulses," *Jpn. J. Appl. Phys.* **9**(11), 1361–1371 (1970).
5. G. Mourou, C. V. Stancampiano, A. Antonetti, and A. Orszag, "Picosecond microwave pulses generated with a subpicosecond laser-driven semiconductor switch," *Appl. Phys. Lett.* **39**(4), 295–296 (1981).
6. D. H. Auston, K. P. Cheung, and P. R. Smith, "Picosecond photoconducting Hertzian dipoles," *Appl. Phys. Lett.* **45**(3), 284–286 (1984).
7. P. R. Smith, D. H. Auston, and M. C. Nuss, "Subpicosecond photoconducting dipole antennas," *IEEE J. Quantum Electron.* **24**(2), 255–260 (1988).
8. Ch. Fattinger and D. Grischkowsky, "Terahertz beams," *Appl. Phys. Lett.* **54**(6), 490–492 (1989).
9. N. Katzenellenbogen and D. Grischkowsky, "Efficient generation of 380 fsec pulses of THz radiation by ultrafast laser pulse excitation of a biased metal semiconductor interface," *Appl. Phys. Lett.* **58**(3), 222–224 (1991).
10. B. B. Hu, X.-C. Zhang, D. H. Auston, and P. R. Smith, "Free-space radiation from electrooptic crystals," *Appl. Phys. Lett.* **56**(6), 506–508 (1990).
11. B. Ferguson and X.-C. Zhang, "Materials for terahertz science and technology," *Nat. Mater.* **1**, 26–33 (2002).
12. G. Zhao, R. N. Schouten, N. Van Der Valk, W. Th. Wenckebach, and P. C. M. Planken, "Design and performance of a THz emission and detection setup based on a semi-insulating GaAs emitter," *Rev. Sci. Instrum.* **73**(4), 1715–1719 (2002).
13. P. C. M. Planken, C. E. van Rijmenam, and R. N. Schouten, "Optoelectronic pulsed THz systems," *Semicond. Sci. Technol.* **20**(7), S121–S127 (2005).
14. T-Ray Science Inc., T-Lux2009 Catalogue, <www.t-rayscience.com>

15. Y. R. Shen, *The Principles of Nonlinear Optics*, Wiley, Hoboken, NJ (1984).
16. C. A. Schmuttenmaer, "Exploring dynamics in the far-infrared with terahertz spectroscopy," *Chem. Rev.* **104**(4), 1759–1779 (2004).
17. R. Huber, A. Brodschelm, F. Tauser, and A. Leitenstorfer, "Generation and field-resolved detection of femtosecond electromagnetic pulses tunable up to 41 THz," *Appl. Phys. Lett.* **76**(22), 3191–3193 (2000).
18. B. Yu, F. Zeng, Y. Yang, Q. Xing, A. Chechin, X. Xin, I. Zeylikovich, and R. R. Alfano, "Torsional vibrational modes of Tryptophan studied by terahertz time-domain spectroscopy," *Biophys. J.* **86**(3), 1649–1654 (2004).
19. B. L. Yu, Y. Yang, F. Zeng, X. Xin, and R. R. Alfano, "Reorientation of H_2O cage studied by terahertz time-domain spectroscopy," *Appl. Phys. Lett.* **86**(6), 061912 (2005).
20. B. L. Yu, Y. Yang, F. Zeng, X. Xin, and R. R. Alfano, "Terahertz absorption spectrum of D_2O vapor," *Opt. Commun.* **258**(2), 256–263 (2006).
21. X. Xin, H. Altan, A. Saint, D. Matten, and R. R. Alfano, "Terahertz absorption spectrum of para and ortho water vapor at different humidities at room temperature," *J. Appl. Phys.* **100**(9), 094905 (2006).
22. B. L. Yu, B. F. Zeng, Q. Xing, and R. R. Alfano, "Probing dielectric relaxation properties of liquid CS_2 with terahertz time-domain spectroscopy," *Appl. Phys. Lett.* **82**(26), 4633–4635 (2003).
23. B. L. Yu, Y. Yang, F. Zeng, X. Xin, and R. R. Alfano, "Direct observation of coherent rotational excitation, dephasing and depopulation of methanol and its isotopes using THz pulse radiation," *Appl. Phys. Lett.* **86**(10), 101108 (2005).
24. H. Altan, B. Yu, S. A. Alfano, and R. R. Alfano, "Terahertz (THz) spectroscopy of Freon-11 (CClF, CFC-11) at room temperature," *Chem. Phys. Lett.* **427**(4–6), 241–245 (2006).
25. B. Yu, A. Alimova, A. Katz, and R. R. Alfano, "THz absorption spectrum of Bacillus subtilis spores," *Proc. SPIE* **5727**, 20–23 (2005).
26. B. Yu, F. Zeng, V. Kartazayev, and R. R. Alfano, "Terahertz studies of the dielectric response and second-order phonons in a GaSe crystal," *Appl. Phys. Lett.* **87**(18), 182104 (2005).
27. H. Altan, X. Xin, D. Matten, and R. R. Alfano, "Direct observation of the strength of plasmon-longitudinal optical phonon interaction in n-type GaAs," *Appl. Phys. Lett.* **89**(5), 052110 (2006).
28. A. J. Campillo, R. C. Hyer, and S. L. Shapiro, "Broadly tunable picosecond infrared source," *Opt. Lett.* **4**(10), 325–327 (1979).
29. A. J. Campillo, R. C. Hyer, and S. L. Shapiro, "Broadly tunable picosecond IR source," U.S. Patent No. 4, 349,907 (1982).
30. K. M. Evenson, D. A. Jennings, and F. R. Petersen, "Tunable far-infrared spectroscopy," *Appl. Phys. Lett.* **44**(6), 576–578 (1984).
31. W. Shi, M. Leigh, J. Zong, and S. Jiang, "Single-frequency terahertz source pumped by Q-switched fiber lasers based on difference-frequency generation in GaSe crystal," *Opt. Lett.* **32**(8), 949–951 (2007).
32. K. Miyamoto, S. Ohno, M. Fujiwara, H. Minamide, H. Hashimoto, and H. Ito, "Optimized terahertz-wave generation using BNA-DFG," *Opt. Express* **17**(17), 14832–14838 (2009).
33. K. Kawase, T. Hatanaka, H. Takahashi, K. Nakamura, T. Taniuchi, and H. Ito, "Tunable terahertz-wave generation from DAST crystal by dual signal-wave parametric oscillation of periodically poled lithium niobate," *Opt. Lett.* **25**(23), 1714–1716 (2000).
34. A. Raman, "Dendrimer waveguide based high-efficiency terahertz source," *Proc. SPIE* **6893**, 689302 (2008).
35. E. R. Mueller, "Submillimeter wave lasers," in *Wiley Encyclopedia of Electrical and Electronics Engineering*, J. G. Webster (Ed.), Vol. 20, pp. 597–615, Wiley, Hoboken, NJ (1999).
36. E. R. Mueller, J. Fontanella, and R. W. Henschke, "Stabilized, integrated, far-infrared laser system for NASA/Goddard Space Flight Center," in *Proc. of 11th Int. Symp. Space Terahertz Technol.*, May 1–3, Ann Arbor (2000).
37. F. Capasso, C. Sirtori, and A. Y. Cho, "Coupled quantum well semiconductors with giant electric field tunable nonlinear optical properties in the infrared," *IEEE J. Quantum Electron.* **30**(5), 1313–1326 (1994).
38. J. Faist, F. Capasso, D. L. Sivco, C. Sirtori, A. L. Hutchinson, and A. Y. Cho, "Quantum cascade laser," *Science* **264**(5158), 553–556 (1994).
39. R. Kohler, A. Tredicucci, F. Beltram, H. E. Beere, E. H. Linfield, A. G. Davies, D. A. Ritchie, R. C. Lotti, and F. Rossi, "Terahertz semiconductor-heterostructure laser," *Nature* **417**(9 May), 156–159 (2002).
40. B. S. Williams, S. Kumar, Q. Hu and J. L. Reno, "Operation of terahertz quantum-cascade lasers at 164 K in pulsed mode and at 117 K in continuous-wave mode," *Opt. Express* **13**(9), 3331–3339 (2005).
41. B. S. Williams, S. Kumar, Q. Hu, and J. L. Reno, "High power terahertz quantum-cascade lasers," *Electron. Lett.* **42**(2), 89–91 (2006).
42. B. S. Williams, "Terahertz quantum-cascade lasers," *Nat. Photon.* **1**(9), 517–525 (2007).
43. L. Diehl, D. Bour, S. Corzine, J. Zhu, G. Hofler, M. Loncar, M. Troccoli, and F. Capasso, "High temperature continuous wave operation of strain-balanced quantum cascade lasers grown by metal organic vapor-phase epitaxy," *Appl. Phys. Lett.* **89**(8), 081101 (2006).
44. Q. J. Wang, C. Pflugl, L. Diehl, F. Capasso, S. Faruta, and H. Kan, "High-power long-wavelength room-temperature MOVPE-grown quantum cascade lasers with air-semiconductor waveguide," *Electron. Lett.* **44**(8), 525–526 (2008).
45. S. Katz, A. Vizbaras, G. Boehm, and M. C. Amann, "Injectorless quantum cascade laser operating in continuous wave above room temperature," *Semicond. Sci. Technol.* **24**(12), 122001 (2009).
46. M. A. Belkin, F. Capasso, A. Belyanin, D. L. Sivco, A. Y. Cho, D. C. Oakley, C. J. Vineis, and G. W. Turner, "Terahertz quantum-cascade-laser source based on intracavity-difference frequency generation," *Nat. Photon.* **1**(5), 288–292 (2007).
47. E. Brundermann, D. R. Chamberlin, and E. E. Haller, "High duty cycle and continuous terahertz emission from germanium," *Appl. Phys. Lett.* **76**(21), 2991–2993 (2000).
48. A. Bergner, U. Heugen, E. Brundermann, G. Schwaab, M. Havenith, D. R. Chamberlin, and E. E. Haller, "New p-Ge THz laser spectrometer for the study of solutions: THz absorption spectroscopy of water," *Rev. Sci. Instrum.* **76**(6), 063110 (2005).
49. H.-W. Hubers, S. G. Pavlov, and V. N. Shastin, "Terahertz lasers based on germanium and silicon," *Semicond. Sci. Technol.* **20**, S211–221 (2005).
50. E. Brunderman, "Widely tunable far-infrared hot-hole semiconductor lasers," Chapter 6 in *Long-Wavelength Infrared Semiconductor Lasers*, H. K. Choi (Ed.), pp. 279–350, Wiley, Hoboken, NJ (2004).
51. M. Tonouchi, "Cutting-edge terahertz technology," *Nat. Photon.* **1**(2), 97–105 (2007).
52. S. Ebbinghaus, S. J. Kim, M. Heyden, X. Yu, U. Heugen, M. Gruebele, D. M. Leitner, and M. Havenith, "An extended dynamical hydration shell around proteins," *Proc. Natl. Acad. Sci. USA* **104**(52), 20749–20752 (2007).
53. B. Born and M. Havenith, "Terahertz dance of protein and sugars with water," *J. Infrared Milli. Terahz. Waves* **30**(12), 1245–1254 (2009).
54. P. P. Ho and R. R. Alfano, "Optical Kerr effect in liquids," *Phys. Rev. A* **20**(5), 2170–2187 (1979).
55. N. Laman, S. S. Harsha, D. Grischkowsky, and J. S. Melinger, "High-resolution waveguide THz spectroscopy of biological molecules," *Biophys. J.* **94**(3), 1010–1020 (2008).